INSTITUTE OF PHYSICS PUBLISHING SUPERCONDUCTOR SCIENCE AND TECHNOLOGY

Supercond. Sci. Technol. **18** (2005) 1502–1505 doi:10.1088/0953-2048/18/11/016

# Enhancement of flux pinning in $YBa_2Cu_3O_{7-\delta}$ thin films embedded with epitaxially grown $Y_2O_3$ nanostructures using a multi-layering process

**A A Gapud[1,2,4], D Kumar[2,3], S K Viswanathan[3], C Cantoni[2], M Varela[2], J Abiade[3], S J Pennycook[2] and D K Christen[2]**

[1] Department of Physics, University of South Alabama, Mobile, AL 36688, USA
[2] Oak Ridge National Laboratory, Oak Ridge, TN 37831, USA
[3] North Carolina A&T State University, Greensboro, NC 27411, USA

E-mail: gapud@usouthal.edu

Received 28 July 2005, in final form 23 September 2005
Published 7 October 2005
Online at stacks.iop.org/SUST/18/1502

**Abstract**
Nanodot arrays of $Y_2O_3$ were dispersed in thin films of $YBa_2Cu_3O_{7-\delta}$ (YBCO) by growing alternating layers of these two species using a pulsed laser deposition method. As a result, critical current density $J_c$ both in applied magnetic field and self-field is enhanced by as much as an order of magnitude, along with a significant increase in the irreversibility field $H_{irr}$. High-resolution scanning transmission electron microscopy (STEM) and $Z$-contrast STEM show that the nanoparticles are crystalline and coherent with the YBCO matrix. Whereas in most other studies pinning has been attributed to the *strain* fields around the nanoparticles, in this case pinning may actually be due to the nanoparticles *themselves*, since the delineation between the two species is very sharp and STEM reveals no discernible strain fields in the superconducting material around the nanoparticles.

(Some figures in this article are in colour only in the electronic version)

The enhancement of critical current density $J_c$ in films of high-temperature superconductor $YBa_2Cu_3O_x$ (YBCO) has attracted renewed interest, spurred by the development of second-generation 'coated conductor' films for power applications [1]. Previous methods that were used to controllably produce flux-pinning defects, such as heavy-ion irradiation, are not deemed viable for large-scale, long-length or 'reel-to-reel' production of high-$J_c$ films. With the advent of nanostructure processing in recent years came more economical alternatives of modifying the film growth process to introduce nanostructures that perturb the crystal lattice. For films made by pulsed laser deposition (PLD), one may readily take advantage of island growth which could be interrupted before a continuous layer is formed. Processing conditions are then fine-tuned in order to achieve the optimal level of nanoparticle density and size, analogous to optimizing irradiation-induced defects. One particular variant of this involves the deposition of alternating layers of YBCO and a non-reacting oxide that would grow epitaxially with it. This is done by switching targets periodically during the deposition, thus distributing the impurity in alternating layers along the film cross-section. Haugan and co-workers [2, 3] applied this technique to introduce nano-discs of $Y_2BaCuO_5$ (211), which successfully enhanced $J_c$ over a wide range of field orientations. They have also used other oxides that were less successful. One of these is yttria, $Y_2O_3$, which has been used successfully to grow nanostructures in other growth procedures [4, 5]. Attempts by Campbell *et al* [6] at multilayering with this material have been modest at best, as will be discussed below.

Although nanodots of $Y_2O_3$ have been shown to induce additional pinning, this has always been due to *strain* in the

[4] Author to whom any correspondence should be addressed.

**Table 1.** Samples in the study. All films have a total thickness of 130 nm.

| Sample | Nominal thickness of $Y_2O_3$ layer (nm) | Substrate | Temp. (°C)/ Press. (mTorr) | Measure-ments |
|---|---|---|---|---|
| I | 0.50 | LAO | 780/300 | $J_{cM}$ |
| II | 1.0 | STO | 780/300 | $J_{cM}$, TEM |
| III | 2.0 | STO | 780/200 | $J_{cT}$ |
| IV | 2.0 | LAO | 750/200 | $J_{cT}$ |
| V | (Control sample: pure YBCO) | STO | 780/200 | $J_{cT}$ |
| VI | (Control sample: pure YBCO) | STO | 780/200 | $J_{cM}$ |

YBCO lattice as a result of these inclusions. Such strain, however, could have detrimental effects on the YBCO: aside from the thickness dependence of $J_c$, there is also a limitation placed on the thickness at which such films could be grown [7]. The present study succeeded in producing more coherent growth between the two species so that any flux pinning would be induced only by *the nanodots themselves*. The result is an enhancement of the $J_c(B)$ by up to one order of magnitude in moderate magnetic fields $B$, and also in achieving a self-field $J_c(10\ \mathrm{K}) > 80\ \mathrm{MA\ cm^{-2}}$.

Table 1 lists properties of the four samples in this study, labeled I–IV. Included are two pure-YBCO samples V and VI, which were grown under similar conditions. Sample VI was a high-quality film used in a previous study [8], while sample V was grown in the same chamber as samples I–IV. Laser ablation was done at 10 Hz with an energy of 70 mJ at the target of either YBCO or $Y_2O_3$, over a $1 \times 4\ \mathrm{mm}^2$ spot size from a $12 \times 4\ \mathrm{mm}^2$ aperture. Deposition was on single-crystal $SrTiO_3$ or $LaAlO_3$ substrates which were heated in flowing $O_2$ gas, and then cooled naturally in 500 Torr of $O_2$. The $Y_2O_3$ and YBCO targets were mounted on a carousel for switching, rastering, and rotating. The nominal film thickness is based on the number of laser shots on the target. The thickness was calibrated using standard contact profilometry; separate samples were grown on Si with a partially obscuring mask in order to create a measurable step. Using this information, the nominal thicknesses used for the $Y_2O_3$ deposition were 0.5, 1, and 2 nm, while each YBCO spacer layer was maintained at 10 nm. Transport measurements of resistivity, critical temperature $T_c$, and $J_c$ were conducted on samples III and IV using a four-probe method, where currents were applied as 50 ms pulses for levels above 100 mA (maximum attainable current is 40 A) in order to minimize Joule heating from the contact resistance, which was ~0.1 mΩ through a cold indium solder with silver or gold pads deposited on the film. The irreversibility line $H_{irr}$ was determined as the field where the $V(I)$ curve has a power of 2 in the vicinity of the 1 $\mu\mathrm{V\ cm^{-1}}$ criterion for $J_c$; this corresponds to critical current density levels of $\sim 10^3\ \mathrm{A\ cm^{-2}}$. Magnetization measurements on samples I and II were conducted in a Quantum Design MPMS SQUID magnetometer, and the cross-section microstructure of sample II was analysed using an aberration corrected VG Microscopes HB501UX dedicated STEM. X-ray diffractometry was also performed on all four films to determine film crystallinity, and especially to analyse the $Y_2O_3$ diffraction peaks. Films

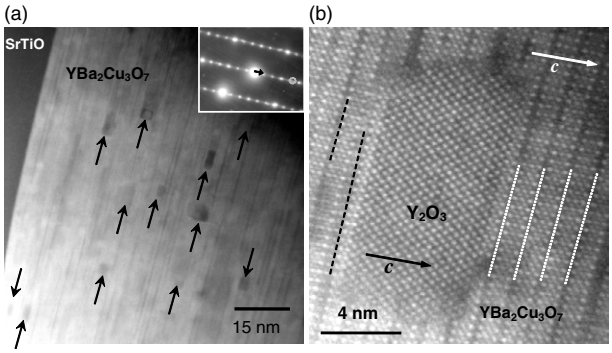


**Figure 1.** Cross-section high-resolution STEM of multilayer film II. (a) Nanoparticles (indicated by arrows) are clearly discernible, with sizes ranging from 3 to 10 nm and about 5 to 20 nm apart. Note the dark fringes (marked by white lines) demarcating the YBCO unit cells ($c = 11.7$ Å), and planar inclusions (marked by dashed black lines). Inset: electron diffraction pattern of this area. The arrow shows the YBCO(001) reflection, while the circle marks the (002) $Y_2O_3$ reflection. (b) High-resolution image of a $Y_2O_3$ nanoparticle, coherent with the YBCO matrix.

with 4 nm $Y_2O_3$ layers were also fabricated, but they were of consistently poor quality, indicating an excess level of $Y_2O_3$ impurity for the processing conditions used.

STEM observations confirm that the $Y_2O_3$ has indeed grown in the form of nanodots. Figure 1(a) is a low magnification image from sample II. The inset of figure 1(a) shows an electron diffraction pattern from this area where the YBCO(001) lattice vector has been highlighted with an arrow, while the $Y_2O_3$(002) reflection has been marked with a circle, showing that they are perfectly aligned with each other. Nanodots in the image have been indicated with arrows, and their size is variable, ranging between 3 and 10 nm.

Figure 1(b) shows a high-resolution $Z$-contrast STEM image of one such $Y_2O_3$ nanodot. For this imaging technique, the lighter atomic columns show up darker, while the heavier columns show an enhanced (brighter) contrast. The $Y_2O_3$ nanoparticles are crystalline and coherent with the YBCO matrix. Actually, the YBCO $c$-axis is parallel to the $Y_2O_3$ nanoparticle $c$-axis, while the (110) axis of $Y_2O_3$ lies parallel to the YBCO $a$ or $b$ directions. In this figure, Y atomic planes in YBCO have been highlighted with white dotted lines, evidencing that the interface runs parallel to the YBCO $ab$-plane, and consists of a Y plane shared between both materials. Furthermore, there is no discernible amorphization of either material; neither is there any obvious sign of strain fields in the YBCO lattice around the particles.

As independent confirmation and comparison with the unembedded nanodot dimensions, we calculated the particle size from x-ray diffraction (XRD) at wavelength $\lambda$ using the Scherrer formula, $t = 0.9\lambda/(\Delta\theta \cos\theta_B)$, which relates $\Delta\theta$, the FWHM of the diffraction peak at $2\theta_B$, with the average size $t$ of crystallites [9]. To do this, we fabricated model systems comprising one layer of $Y_2O_3$ grown on a single YBCO layer which had been deposited on single-crystal LAO. Such samples were grown with $Y_2O_3$ nominal thicknesses of 1 and 2 nm. We then measured the XRD intensity of the $Y_2O_3$ (200) peak. Applying the Scherrer equation yielded $Y_2O_3$ crystallite sizes of ~6 nm *for both thicknesses*. Not only is this consistent with

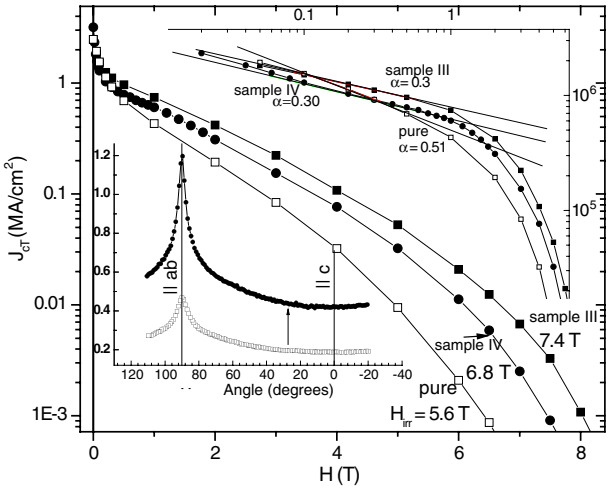


**Figure 2.** Magnetic field dependence of transport critical current density $J_{cT}$ at 77 K for $B \parallel c$ of multilayered film, YBCO/($Y_2O_3$ /YBCO) ×9. At $B = 5$ T, for sample IV and sample III, $J_c$ is enhanced by a factor of at least three and five, respectively. For sample III, the irreversibility field increases by 32% from 5.6 to 7.4 T. Lower inset: dependence of $J_{cT}$ on orientation angle of the field relative to the $c$ direction (maximum Lorentz configuration) for sample IV, showing a uniform increase in $J_{cT}$ over all angles measured. Upper inset: for the field regime where $J_c(B) \sim B^{-\alpha}$ in both cases $\alpha$ decreases by 33%.

the TEM results; it also strongly implies that $Y_2O_3$ content in this range makes little difference in the particle size, nor does the additional step of embedding the nanoparticles within the YBCO matrix.

Transport $J_{cT}$ versus field $B$ at 77 K for samples III and IV, which had the thickest $Y_2O_3$ at 2 nm, is shown in figure 2. Also included are data for sample V, a pure-YBCO film that was grown in the same chamber and under similar conditions. All samples had a slightly degraded $T_c$ of 89 K, but no correlation with nominal $Y_2O_3$ thickness was found. The enhancement in $J_c(B)$ is quite significant, a factor of three for multilayers on LAO and a factor of five for multilayers on STO, at $B = 5$ T. Another clear indicator that flux pinning has been enhanced is the upward shift of the irreversibility field $H_{irr}$, at which $J_c$ is defined to be negligible due to flux motion. The irreversibility fields are increased from 5.6 to 6.8 T and 7.4 T.

The dependence of $J_{cT}$ on the orientation of the applied magnetic field gives additional insight as to the nature of the flux pinning. The lower inset of figure 2 shows the data for samples IV and V, at 77 K and 2 T. Both curves are very typical of random pinning [10, 11]: specifically, the absence of any 'peak' for orientations about the direction of the $c$ axis clearly shows that there is no correlation or preferential direction for the pinning or, therefore, of the pinning defects themselves. This would be consistent with a homogeneous distribution of $Y_2O_3$ nano-inclusions if indeed these are the pinning defects. Therefore improvement in pinning is fairly isotropic and enhancement in $J_{cT}$ occurs over a wide range of field orientations. (The result is similar for sample III.) One additional feature of note is that for both samples III and IV the 'peak' in the vicinity of the $a/b$ axis orientation is significantly higher: $J_{cT}(90°)/J_{cT}(0°)$ is about 3.0 for the multilayered sample, while for the control sample this ratio is closer to 2.5. This would be consistent with the presence of planar defects, as marked in figure 1, most likely intergrowths of copper-rich Y-248 phase. An excess level of yttrium and/or yttrium oxide could have such an effect.

Another indicator of the flux pinning mechanism is in the power-law exponent $\alpha$ for the low-field regime (usually ~0.1–1 T at 77 K) where $J_c(B) \sim B^{-\alpha}$. The value of $\alpha$ is simply the slope for the linear regime in this range of fields, as seen in the log–log plot in the right-hand inset of figure 2. For the pure-YBCO film, $\alpha$ is about 1/2, which is typically observed for PLD growth. According to a model by Nelson and Vinokur [12], for fields above some 'matching' field, $\alpha = 1/2$ is consistent with flux lines shearing past pinned bundles, implying a relatively dilute distribution of extended pinning defects. This is consistent with the expected growth of linear defects as a consequence of island growth for films grown by laser ablation [13]. (Note: while this may seem inconsistent with the results of field-orientation dependence of $J_c$ in figure 2, lower inset, it should be pointed out that the latter was measured at 2 T, well above the power-law regime.) With the introduction of $Y_2O_3$ layers, the field dependence of $J_{cT}$ is weakened noticeably: $\alpha$ is reduced to 0.30, which would be consistent with more efficient pinning (less field dependence). While there is a model by Ovchinnikov and Ivlev [14] predicting $\alpha \sim 0.6$ for the case of uncorrelated, strong but dilute pinning sites—and which was observed in a recent study involving nano-inclusions in *ex situ* grown YBCO film [5]—there is as yet no reported model for $\alpha \sim 0.3$, as far as we know. However, this low value of power-law exponent has been observed in other very strong-pinning systems comprising nanoprecipitates in YBCO [15, 16].

There is even improvement at self-field or $B = 0$, where the $J_c$ of sample III is increased up to 3.4 MA cm$^{-2}$, from 2.5 MA cm$^{-2}$ for sample V. For sample IV on STO there is no enhancement, but the fact that the self-field $J_c$ was not degraded is noteworthy, considering that impurities had been added to the YBCO. Although at such very low flux densities in self-field the pinning may be sufficient to make any dissipative flux flow highly unlikely, the defects could also impede the percolative flow of supercurrent.

The transport current results are consistent with the magnetization critical current density $J_{c,M}(B)$ measured at lower fields for samples I and II, which had the nominally thinner $Y_2O_3$ layers at 0.5 and 1 nm, respectively. The latter is clearly superior, as shown in figure 3. Included here are data for a high-quality, pure sample (open circles). At temperatures down to 10 K, the multilayer samples have significantly higher $J_{cM}$ in field, increasing by an order of magnitude for the sample with 1 nm $Y_2O_3$ layers at fields close to 1 T. Note that at 10 K $J_c$ reaches a maximum of more than 80 MA cm$^{-2}$. Interestingly, the improvement is greater towards lower temperatures. In addition, when the $Y_2O_3$ nominal thickness is increased twofold in this case, the $J_c$ also increases about twofold, almost uniformly over the entire range of fields $B$. This might be consistent if there were a twofold increase in the density of nanodots as result of twofold increase in the number of laser ablation pulses (all other parameters unchanged). The alternative possibility of an enhancement of pinning strength of each nanodot is less likely: recall that the Scherrer equation showed little change in nanodot size with respect to number of laser shots of $Y_2O_3$.

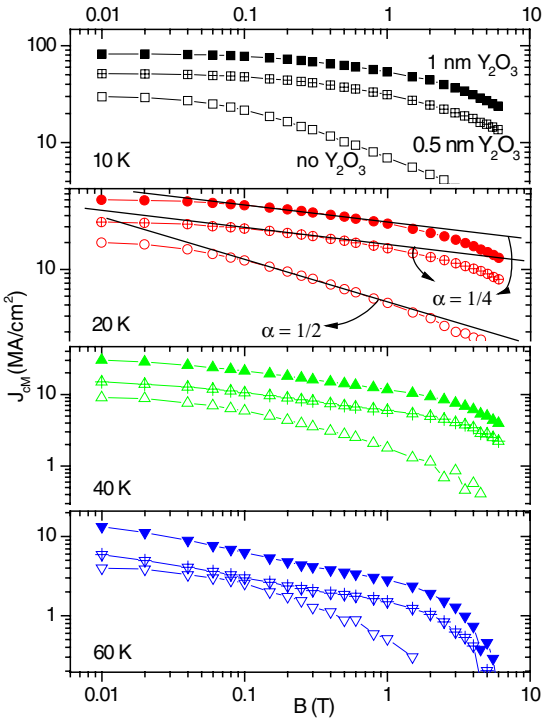


**Figure 3.** Enhancement of magnetization $J_c(B)$ in multilayer films at four different temperatures. The addition of nominally 0.5 nm $Y_2O_3$ layers increases $J_c$ in moderate fields $B$ by at least a factor of two, with greater improvement at lower temperatures. For the 1 nm $Y_2O_3$ layers, the enhancement is by at least another factor of two over the 0.5 nm case and as much as an order of magnitude over the pure films. Both multilayer films have a smaller linear-regime exponent $\alpha$ relative to the control sample, indicating a change in pinning mechanism. Between the two multilayer films, $\alpha$ is the same, implying no change in the pinning mechanism when the $Y_2O_3$ layer nominal thickness is doubled.

As with the transport $J_c$ data of figure 2, the magnetization $J_c$ data are plotted on a log–log scale in order to analyze the linear regime where $J_c \sim B^{-\alpha}$, and the $\alpha$ values are consistent: again, the pure YBCO shows the value $\alpha \sim 1/2$, while for the multilayer films $\alpha$ varies from 1/4 to 1/3 with temperature.

It is important to compare all these results with those from the very similar work of Campbell *et al* [6] in which PLD multilayering of $Y_2O_3$ was also executed. In that work, there was a clear indication of a threshold upper nominal thickness of 0.7 nm for the $Y_2O_3$ layers, above which their $J_{cM}$ was found to deteriorate. Our results indicate that the best $J_{cM}$ is obtained at 1.0 nm, and becomes worse above ~4.0 nm nominal thickness; considering possible uncertainties in the thickness calibration, this finding is comparable and qualitatively consistent with the Campbell results. However, we do not observe the improvement with the thinner, 0.5 nm layer but instead see consistently smaller $J_{cM}$. Also, while the two studies show similarly high values of $J_c$ at self-field, in the previous study the enhancement of in-field $J_{cM}$ at 77 K was modest at best, and only at highest fields. This difference could be attributed to the fact that the previous study involved *much larger nanoparticles*, with an *average* diameter of 12.9 nm for the 1.4 nm nominal thickness, almost twice the average size of those in this present study (closer to 6 nm). This may be because the PLD processing in the present study used *identical* laser energies for the two targets, while in the other study a much lower energy was used for ablating the $Y_2O_3$ target; therefore even with similar nominal thickness the difference would be expected to manifest in terms of island size. The difference in the resulting lateral size of the nanoparticles may have a significant impact on the amount of long-range strain in the YBCO lattice—of which they also showed evidence—which would fail to significantly improve the overall critical current. In the present work, there is no evidence of strain, and so a similar density of smaller $Y_2O_3$ nanoparticles may be providing the YBCO much more superconducting phase for the percolation of supercurrent. Another possibility is that a larger-area pinning site could allow for more dissipative flux motion than a smaller-area one, providing another avenue for $J_c$ degradation.

To summarize, using pulsed laser deposition in a multilayering scheme, we have inserted coherent crystallite $Y_2O_3$ nanodots within well formed and *non-strained* YBCO thin films on single-crystal substrates, resulting in as much as a tenfold increase in critical current density in applied magnetic fields, as well as in self-field, reaching a very high value of 81 MA cm$^{-2}$ at 10 K.

## Acknowledgments

This work is part of a Nanoscale Interdisciplinary Team funded by NSF (grant number DMR/CMP-0403480) and based at North Carolina A&T State University. Work performed at the Oak Ridge National Laboratory (managed by UT-Battelle, LLC for the USDOE under contract No DE-AC05-00OR22725) was supported by the US Department of Energy's Office of Electricity Distribution and Energy Reliability and Office of Basic Energy Sciences. Special thanks go to S Pai and A O Ijadoula for crucial assistance in film fabrication and in SQUID measurements, respectively.

## References

[1] Larbalestier D, Gurevich A, Feldmann D M and Polyanskii A 2001 *Nature* **414** 368
[2] Barnes P N, Murray P T, Haugan T, Rogow R and Perram G P 2002 *Physica* C **377** 578
[3] Haugan T, Barnes P N, Maartense I, Cobb C B, Lee E J and Sumption M 2003 *J. Mater. Res.* **18** 2618
[4] Matsumoto K, Horide T, Ichinose A, Horii S, Yoshida Y and Mukaida M 2005 *Japan. J. Appl. Phys.* 2 **44** L246
[5] Gapud A A, Feenstra R, Christen D K, Thompson J R and Holesinger T G 2005 *IEEE Trans. Appl. Supercond.* **15** 2578
[6] Campbell T A, Haugan T J, Maartense I, Murphy J, Brunke L and Barnes P N 2005 *Physica* C **423** 1
[7] Wu J Z *et al* 2005 private communication
[8] Thompson J R, Kim H J, Cantoni C, Christen D K, Feenstra R and Verebelyi D T 2004 *Phys. Rev.* B **69** 104509
[9] Cullity B D and Stock S R 2001 *Elements of X-Ray Diffraction* (Upper Saddle River, NJ: Prentice-Hall)
[10] Civale L *et al* 2004 *J. Low Temp. Phys.* **135** 87
[11] Civale L *et al* 2004 *Appl. Phys. Lett.* **84** 2121
[12] Nelson D R and Vinokur V 1993 *Phys. Rev.* B **48** 13060
[13] Dam B *et al* 1999 *Nature* **399** 439
[14] Ovchinnikov Y N and Ivlev B I 1991 *Phys. Rev.* B **43** 8024
[15] Macmanus-Driscoll J L, Foltyn S R, Jia Q X, Wang H, Serquis A, Civale L, Maiorov B, Hawley M E, Maley M P and Peterson D E 2004 *Nat. Mater.* **3** 439
[16] Kang S, Goyal A, Leonard K J, Gapud A A, Varela del Arco M, Paranthaman M P, Martin P M, Ijaduola A O and Thompson J R 2005 *Supercond. Sci. Technol.* submitted